

Effect of Peak Power and Pulse Width on Coherent Doppler Wind Lidar's SNR

REN Yong^{1,2,3}, WU Xuefei^{2,3}, TAO Fa², CAO Haishuai⁴

(1. Fujian Key Laboratory of Severe Weather, Fuzhou 350001; 2. Meteorological Observation Center of the China Meteorological Administration, Beijing 100081; 3. Fujian Atmospheric Detection Technology Support Center, Fuzhou 350008; 4. Qingdao Leice Transient Technology Co. Ltd, Qingdao 266000)

Abstract: The laser device is the core component of coherent Doppler wind lidar. The peak power and pulse width of laser transmitting pulse have important effects on SNR. Based on coherent Doppler wind pulse lidar, the peak power and pulse width influence on SNR is studied on the theoretical derivation and analysis, and the results show that the higher the peak power can realize the greater the signal-to-noise ratio of coherent Doppler wind lidar. But when the peak power is too large, the laser pulse may appear nonlinear phenomenon, which cause the damage of the laser. So, the peak power must be less than the stimulated brillouin scattering power threshold. Increasing the pulse width can make the laser device to output more energy, but it will also make the spatial resolution lower, and the influence of turbulence on SNR will be greater. After a series of simulation analyses, it can be concluded that when the peak power is 650W and the pulse width is 340ns, the SNR of the system can be maximized. In addition, the coherent Doppler wind lidar system is set up to carry out corresponding experimental verification. The experimental results are consistent with the theoretical analysis and simulation, which verifies the correctness of the theoretical analysis and simulation results. It provides theoretical basis and practical experience for the design of laser transmitting pulse in coherent Doppler wind lidar system.

Keywords: Coherent Lidar, Fiber Laser, Peak Power, Pulse Width, Signal-to-Noise Ratio (SNR)

1 Introduction

The atmospheric wind field (AWF) is an important object of research for atmospheric dynamics and climatology. It is also the main driving force for aerosol transport, air-sea exchange, water circulation and climate change. Accurate detection of AWF is of great significance for global climate change and numerical weather prediction^[1]. With high precision, high temporal-spatial resolution, wide-range detection and other advantages in remote sensing of wind speed, the coherent Doppler wind lidar has become one of the important techniques for AWF measurement^[2-5].

For the earliest wind sounding by Doppler lidar, continuous laser was used to measure the echo from clean air. In 1974, the NASA CW 50W carbon dioxide laser system was installed on an aircraft to measure the air velocity at a height of up to 3,000 m^[6]; in 1978, the pulsed lidar was used to provide a two-dimensional (2D) diagram of the horizontal wind field at aircraft flying height; in 1979, there was the first report on the use of the ground-based movable pulsed Doppler lidar for measurement; from 1981 to 1985, the NOAA ground-based pulsed carbon dioxide TEA lidar system demonstrated that the coherent lidar could be moved to different regions and operated successfully under

normal conditions^[7]. In 2002, U.S. Coherent Inc. developed the first commercial coherent lidar WindTracer, which was installed at Hong Kong International Airport. In 2014, Mitsubishi continued to upgrade the coherent lidar by further increasing the transmitting power, realizing a detection range of over 9 km^[8].

In recent years, the coherent Doppler wind lidar has tended to be increasingly characterized by miniaturization, commercialization, long range and high temporal-spatial resolution^[9]. To achieve a longer measuring range and higher temporal-spatial resolution, the relevant companies and research institutes have devoted themselves to boosting the transmitting power, increasing the optical aperture and improving the signal detection capability. However, there has been very few studies on how seriously the signal-noise ratio (SNR) of lidar is affected by peak power and pulse width. Furthermore, the choice of peak power and pulse width has an important influence on SNR. Therefore, a related study and analysis is conducted in this paper, where a method is also proposed for determining peak power and pulse width. Using this method can select the optimal laser peak power and pulse width, maximizing signal-to-noise ratio of the device under the same conditions, to achieve further measuring distance and higher resolution of space and time, reducing the volume and power consumption of equipment, maximizing economic benefit of laser. And the method can be used for reference in the design of lidar transmitting system.

2 Theoretical Analysis of the SNR of Coherent Doppler Wind Lidar

2.1 Basic Principles of Coherent Doppler Wind Lidar

Fig.1 shows a structural schematic diagram of the coherent Doppler wind lidar. After the seed laser 1 passes through the optical splitter 2, a small part goes to the multi-mode 2×2 coupler for frequency mixing; the other part passes through the optical switch 3 and the frequency shifter 4, and is converted to frequen-

cy-shift pulsed light; then it enters the optical fiber amplifier 5 for power amplification, and is converted to single-frequency mono-pulse transmitted laser. Then, it passes through the multi-mode circulator 6 and the telescope 7 before being transmitted to the target. The backscattered light containing wind speed information is frequency-mixed with local oscillator laser in the multi-mode 2×2 coupler 8, generating a low-frequency beat signal, which enters the balanced detector 9, where it is converted into an electrical signal. The beat-frequency electrical signal is collected and processed by a high-speed analog-to-digital conversion acquisition card to obtain signal spectrum data and radial wind speed, and the wind vector is inverted, too. After signal processing, the results are input to the communication module and the control module through the upper computer.

The SNR of the coherent Doppler wind lidar with the structure shown in Fig.1 is as follows^[10-13]

$$\text{SNR}(R) = \frac{\eta_D(R)\lambda P \Delta T \beta K^{2R/1000} \pi D^2}{8hBR^2} \quad (1)$$

where R represents the distance between the lidar and the target; λ represents the laser wavelength; P represents the peak power of the transmitted pulse; ΔT represents pulse width; β represents the atmospheric backscattering coefficient; K represents the atmospheric transmittance; D represents the aperture of the transmitting telescope; h represents Planck's constant; B represents the receiving bandwidth.

$$\eta_D(R) = \frac{\eta_F}{\left\{ 1 + \left(1 - \frac{R}{R_F} \right)^2 \left[\frac{\pi (A_C D)}{4\lambda R} \right]^2 + \left(\frac{A_C D}{2S_0(R)} \right)^2 \right\}} \quad (2)$$

$$S_0(R) = (1.1k^2 R C_n^2)^{-3/5} \quad (3)$$

where η_F represents the transmittance of transmitted laser and local oscillator laser; R_F represents the focal length; S_0 represents the lateral coherence length; A_C represents the telescope aperture correction factor; k represents the wavenumber; C_n^2 represents the structural parameter of atmospheric refractivity.

It can be seen from equation (1), the SNR is directly proportional to the peak power, i.e., the greater the peak power is, the higher the SNR is. However, the

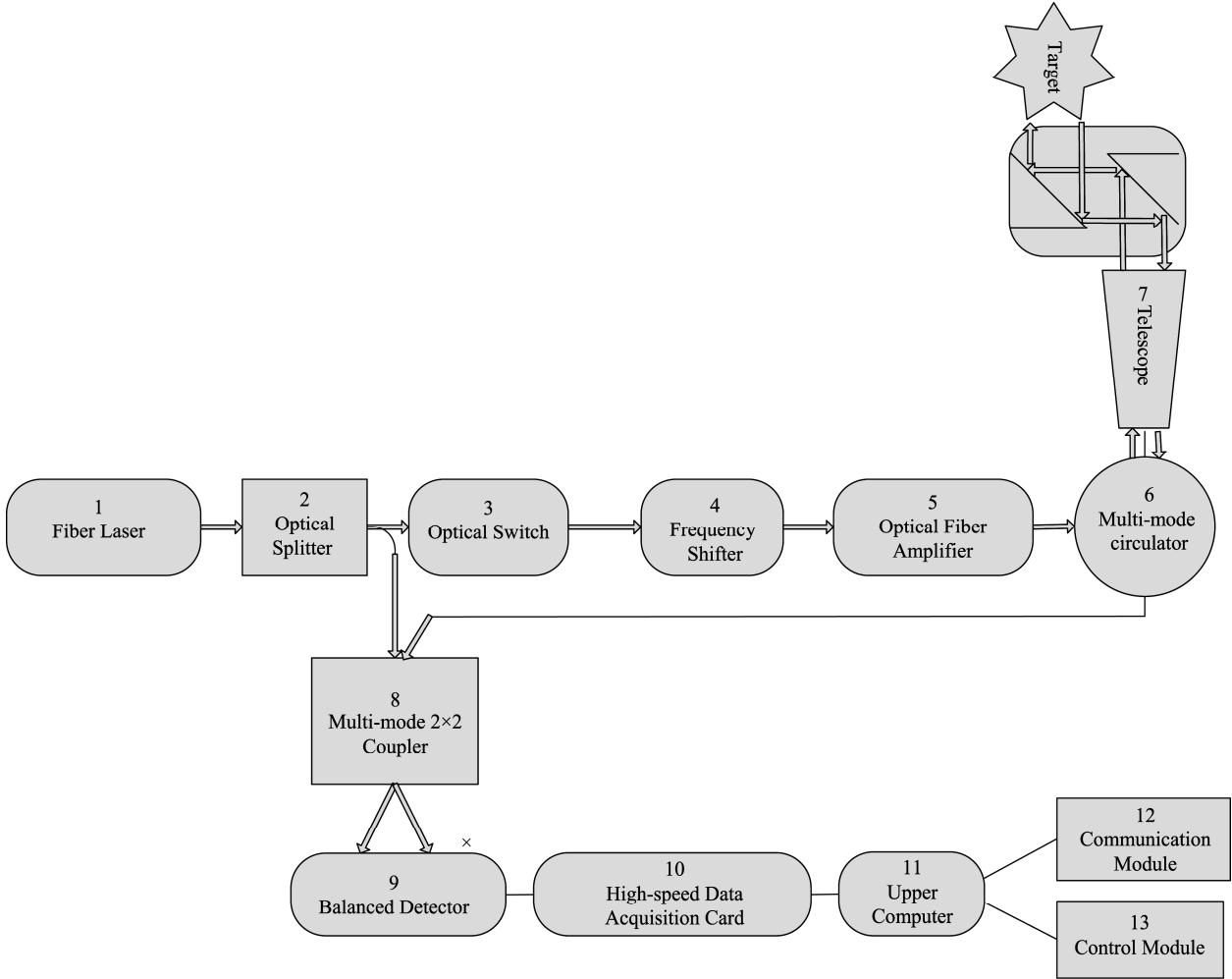


Fig.1 Schematic Diagram of Coherent Lidar's Structure

peak power cannot be increased indefinitely. If the peak power is excessively high, stimulated Brillouin scattering will occur in the light amplifier, thereby seriously affecting the service life the light amplifier. The pulse width ΔT is also directly proportional to the peak power, but excessively wide pulse width will lead to severe turbulence impact on signal, leading to a reduction in the SNR.

2.2 Impact of Stimulated Brillouin Scattering Peak Power

Stimulated Brillouin scattering occurs due to the interaction between incident laser and the acoustic waves in molecules or solids. Light is a kind of electromagnetic wave. When light propagates in a medium, the electromagnetic field exerts an electrostriction

effect on the medium, leading to a constant change in the density of the medium, thus bringing about a periodical change in the refractivity, forming a grating with variable refractivity, so that incident laser is scattered. The power threshold of the incident laser that generates stimulated Brillouin scattering is as follows^[14-15]

$$P_{SBS} = 42 \cdot \frac{1}{g_B} \cdot \frac{\pi r_0^2}{\frac{1}{\alpha} [1 - \exp(-\alpha L)]} \cdot \frac{\Delta \nu_B + \Delta \nu_P}{\Delta \nu_B}$$

Where g_B represents the Brillouin gain coefficient; r_0 represents the radius of the single-mode optical fiber mode field; α represents the optical fiber attenuation coefficient per unit length; L represents the optical fiber length; $\Delta \nu_B$ represents Stimulated Brillouin scattering width; $\Delta \nu_P$ represents incident laser width. Table

1 shows the optical fiber parameters of the laser used. They were substituted into equation (3), obtaining an optical power threshold of 650W. Therefore, it is necessary to ensure that the peak power is lower than 650W when the transmitted pulse of the laser is adjusted.

3 Simulation and Discussion

According to equations (1)-(3), MATLAB was used to simulate and analyze the impact of peak power P on the SNR. The parameters applied in the equations are shown in Table 2. Pulse width modulation (PWM) was set to 300ns while the peak power was continuously increased from 150W to 650W,

and a change curve of the SNR was obtained at 1,000m, as shown in Fig.2. As can be seen from the figure, the SNR increases monotonically with the increasing peak power. When the peak power reaches 650W, the peak power reaches a maximum of 34.4dB.

At the same time, the impact of the pulse width on the SNR was also simulated. Besides, the pulse width was increased from 60ns to 1200ns by simulation, and the change curve of the SNR obtained is shown in Fig.3. As can be seen from the figure, the SNR increases first and then decreases with the increasing pulse width. When the pulse width increases to 340ns, the SNR reaches a maximum of 34.3dB.

Table 1 Symbols and Meanings of System Parameters

Symbols	Meanings	Value	Unit
g_B	Brillouin Gain Coefficient	5	cmGW ⁻¹
r_0	Radius of the Single-mode Optical Fiber Mode Field	11	um
α	Fiber Attenuation Coefficient Per Unit Length	0.2	dB/Km
L	Fiber Length	50	cm
Δv_B	Stimulated Brillouin Scattering Width	100	MHz
Δv_p	Incident Laser Width	100	KHz

Table 2 Symbols and Meanings of System Parameters

Symbols	Meanings	Value	Unit
λ	Wavelength	1.55	um
β	Atmospheric Backscattering Coefficient	4×10^{-7}	m ⁻¹ sr ⁻¹
K	Atmospheric Transmittance	1.7×10^{-4}	m ⁻¹
D	Telescope Aperture	80	mm
h	Planck's Constant	6.626×10^{-34}	J·S
B	Receiving Bandwidth	200	MHz
η_F	Transmittance of Transmitted Laser and Local Oscillator Laser	0.99	
R_F	Focal Length	2000	m
A_C	Telescope Aperture Correction Factor	1	

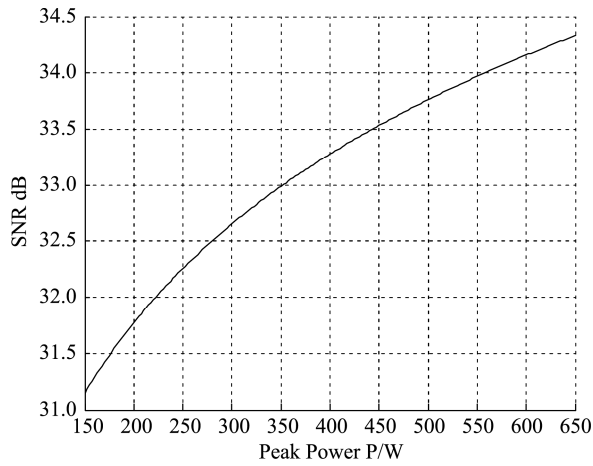


Fig.2 Simulation Change Curve of SNR with Peak Power

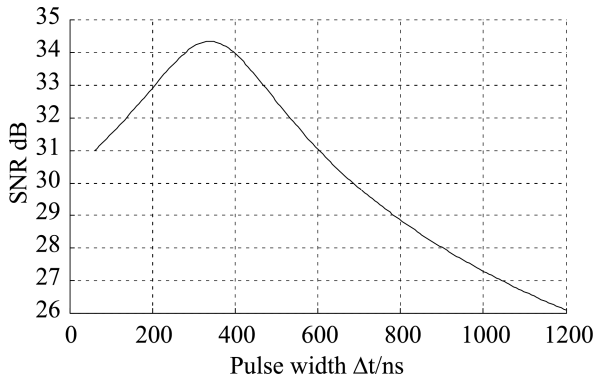


Fig.3 Simulation Change Curve of SNR with Pulse Width

The simulation and analysis of the effects of the peak power and pulse width on the SNR have further deepened the understanding of the previous theoretical analysis. Specifically, the SNR reaches its maximum when the peak power is 650W and the pulse width is 340ns.

4 Validation

According to the schematic diagram of the lidar structure in Fig.1, a specific experimental system was built to verify the simulation results achieved in the previous section. The real object is shown in Fig.4. The well-installed device is shown in Fig.5. The pulse peak power was continuously increased from 150W to 650W by continuously adjusting the laser in Fig.4, in increment of 50W. The SNRs corresponding to peak power conditions are shown by the asterisked curve in Fig.6. As can be seen, the curve obtained in the experiment is in good agreement with the curve obtained by simulation.

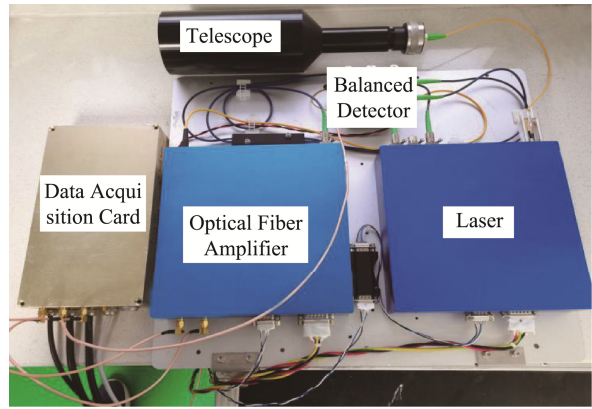


Fig.4 Physical Picture of the Experimental System



Fig.5 Schematic Diagram of the Experimental System

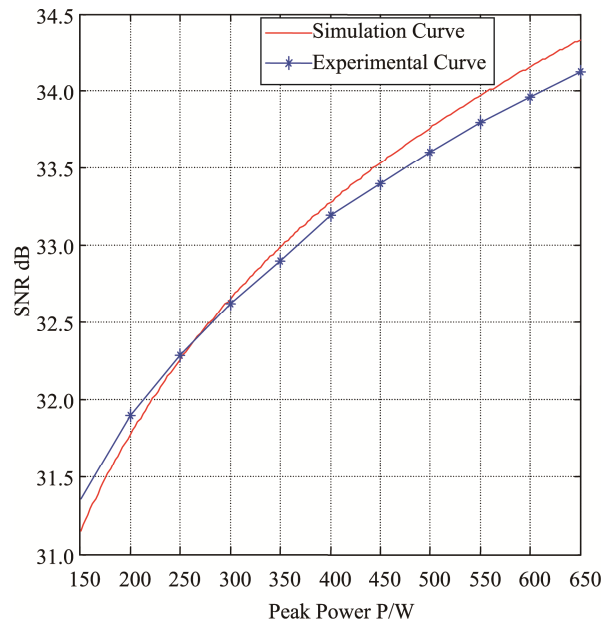


Fig.6 Experimental Change Curve of SNR with Peak Power

The pulse width was continuously increased from 100ns to 1200ns by continuously adjusting the laser in Fig.4, in increments of 50ns. The SNR corresponding to different pulse widths are shown by the asterisked curve in Fig.7. As can be seen, the curve obtained in the experiment is also in good agreement with the curve obtained by simulation. The correctness of the above theoretical analysis and simulation results have been verified by the two experiments.

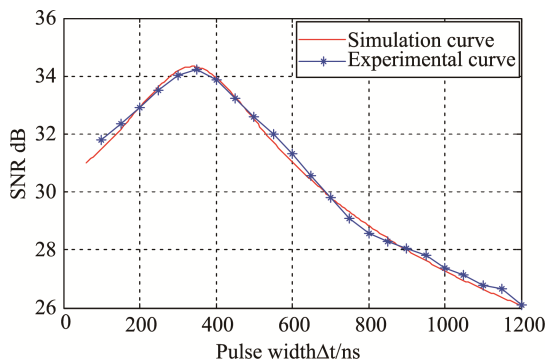


Fig.7 Experimental Change Curve of SNR with Pulse Width

5 Conclusion

This paper has introduced the basic principles of the coherent Doppler wind lidar, derived the SNR formula of the lidar, and analyzed the factors affecting the SNR. The SNR is directly proportional to the peak power of the laser pulse, i.e., the greater the peak power is, the higher the SNR is. However, the peak power cannot be increased indefinitely. If the peak power is excessively high, stimulated Brillouin scattering will occur, thereby causing damage to the lidar. What's more, the lidar will fail to accurately measure the wind speed due to its own frequency shift. Therefore, the peak power must be less than the power threshold generated in the process of stimulated Brillouin scattering. When the peak power is constant, the pulse width can be increased to increase the energy output of the laser. However, the increased pulse width may also reduce the spatial resolution, increasing the influence of turbulence on the signal. Simulation and validation were performed on the basis of the above theoretical

analysis. The results show that the SNR can reach its maximum when the peak power is 650W and the pulse width is 340ns.

References

- [1] Jin X M. (2020). Application research of laser coherent wind technology. *Journal of Atmospheric and Environmental Optics*, 15(3). pp. 161-172.
- [2] Jiang S. (2019). Design and test of laser anemometer based on continuous wave coherence detection. *Infrared and Laser Engineering*, 48(12). pp. 1203008.
- [3] Zhou Y Z. (2019). Research progress and application of coherent wind lidar. *Laser & Optoelectronics Progress*, 56(2). pp. 020001.
- [4] Luo J. (2020). Advances in coherent laser wind measurement technology. *Chinese Journal of Quantum Electronics*, 37(2). pp. 129-137.
- [5] Wang J. (2019). Development of a portable dual field of view mie scattering Lidar. *Chinese Journal of Scientific Instrument*, 40(2). pp. 148-154.
- [6] Köpp F. (1984). Remote measurements of boundary-layer wind profile using a CW Doppler lidar. *Journal of Applied Meteorology*, 23(1). pp. 148-154.
- [7] Hall F F. (1984). Wind measurement accuracy of NOAA pulsed infrared Doppler lidar. *Applied Optics*, 23(15). pp. 2503-2506.
- [8] Hommema. (2003). Packet structure of surface eddies in the atmospheric boundary layer. *Boundary-Layer Meteorology*, 106(1). pp. 147-170.
- [9] Wang X T. (2011). The research of All-fiber laser heterodyne detection for velocity measurement. M Se. Ocean University of China.
- [10] Sonnenschein C M. (1971). Signal-to noise relationships for coaxial systems that heterodyne backscatter from the atmosphere. *Applied Optics*, 10. pp.1600-1604.
- [11] Frehlich R G. (1991). Coherent laser radar performance for general atmospheric refractive turbulence. *Applied Optics*, 30. pp.5325-5352.
- [12] Kong Y X. (2017). Influence of laser linewidth on the performance of space coherent optical communication system. *Chinese Journal of Scientific Instrument*, 38(7).

pp.1668-1674.

- [13] Frehlich R G. (1999). Coherent doppler lidar signal spectrum with wind turbulence. *Applied Optics*, 38, pp.7456–7466.
- [14] Qian S X. (2001). The principles and advances of non-linear optics. *Shanghai: Fudan University Press*, pp.170-178.
- [15] Liu T. (2012). *Research for SBS threshold enhanced in single-mode fiber*. M Se. Huazhong University of Science and Technology.

Author Biographies



REN Yong received a M.Sc. degree and is now a senior engineer. His main research interest includes application research of atmospheric detection technology.

E-mail: 56914200@qq.com



TAO Fa received a Ph.D. degree and is now a senior engineer. His main research interest includes atmospheric sounding technology.

E-mail: Taofa@163.com



Copyright: © 2022 by the authors. This article is licensed under a Creative Commons Attribution 4.0 International License (CC BY) license (<https://creativecommons.org/licenses/by/4.0/>).